Journal of the European Ceramic Society 21 (2001) 471–475

www.elsevier.com/locate/jeurceramsoc

Slow crack growth behavior in Si_3N_4 sintered with $Yb_2Si_2O_7$ tie-line composition additives

Heon-Jin Choi [a], Hyeong-Jong Kim [a], June-Gunn Lee [a], Young-Wook Kim [b,*]

[a] *Multifunctional Ceramics Research Center, Korea Institute of Science and Technology, Seoul 130-650, South Korea*
[b] *Department of Materials Science and Engineering, University of Seoul, Seoul 130-743, South Korea*

Received 1 June 2000; received in revised form 18 July 2000; accepted 31 July 2000

Abstract

Slow crack growth behavior of two gas pressure sintered Si_3N_4 ceramics with different additives; a $Yb_2Si_2O_7$ composition and an Al_2O_3–Y_2O_3 composition, was investigated by constant stress-rate (''dynamic fatigue'') testing at 1400°C. The slow crack growth parameter, n, was 14.7 and 6.3 for Si_3N_4 with $Yb_2Si_2O_7$ and Al_2O_3–Y_2O_3 compositions, respectively. Superior crack growth resistance of Si_3N_4 with $Yb_2Si_2O_7$ composition was due to its higher refractoriness of intergranular glassy films, compared to Si_3N_4 with Al_2O_3–Y_2O_3 composition.

Keywords: Engine components; Grain boundaries; Si_3N_4; Sintering additives; Thermal properties

1. Introduction

Si_3N_4 ceramics are densified by liquid phase sintering using metal oxides as sintering additives. The oxides form an oxynitride melt during sintering and remain at grain boundary as an intergranular glassy film (IGF) after sintering. Presence of the residual IGF leads to the degradation of high temperature properties.[1,2] Several attempts to optimize high temperature properties have been investigated, including the crystallization of the IGF by a post heat treatment,[3] the formation of a transient liquid phase sintering,[4] and the reduction of the overall additive content in combination with the use of refractive additives.[5,6]

Work performed by Lange et al.[7] on the Si_3N_4–SiO_2–Y_2O_3 system has shown that the high temperature properties of Si_3N_4 can be improved by choosing compositions in the Si_3N_4–Si_2N_2O–$Y_2Si_2O_7$ compatibility triangle, since the Si_2N_2O and $Y_2Si_2O_7$ phases are in equilibrium with SiO_2, the oxidation product of Si_3N_4. Lange[8] also proposed similar behavior for compositions in the Si_3N_4–SiO_2–CeO_2 system. On this basis, various rare-earth oxides have been studied as potential sintering additives and verified as effective as Y_2O_3 in the densification of Si_3N_4.[3,9,10] Furthermore, refractory disilicate, $Re_2Si_2O_7$ (Re refers to the cation of a rare earth oxide), can be crystallized at grain boundaries, thereby resulting in improved high temperature properties.[3,11–13] These results make the Si_3N_4–$Re_2Si_2O_7$ tie-line composition attractive for high temperature application of Si_3N_4.

Among the Si_3N_4–SiO_2–Re_2O_3 systems, we have shown that Si_3N_4–$Yb_2Si_2O_7$ composition is one of the best candidates for better high temperature application because of its good flexural strength and oxidation resistance.[14,15] In this study, we characterized slow crack growth (SCG) behavior, that is important to estimate the service life at elevated temperatures, of Si_3N_4 with $Yb_2Si_2O_7$ composition by using constant stress-rate (''dynamic fatigue'') testing at 1400°C and compared to that of Si_3N_4 with 2 wt.% Al_2O_3–4 wt.% Y_2O_3 composition.

2. Experimental procedure

Commercially available Si_3N_4 (SN E-10, Ube Industries, Tokyo, Japan), Yb_2O_3, Y_2O_3 (99.9%, Johnson Matthey, Seabrook, NH, USA), SiO_2 (99.9%, Aerosil 200, Degussa Co., NJ, USA), and Al_2O_3 (99.99%, AKP 30, Sumitomo Chemicals, Tokyo, Japan) powders were

* Corresponding author. Tel.: +82-2-2102760; fax: +82-2-2155863.
E-mail address: ywkim@uoscc.uos.ac.kr (Y.-W. Kim).

0955-2219/01/$ - see front matter
PII: S0955-2219(00)00218-1

used as starting materials. Two compositions, designated as SNYb and SNAY, were prepared corresponding to Si_3N_4 (94 wt.%)–Yb_2O_3 (4.6 wt.%)–SiO_2 (1.4 wt.%) and Si_3N_4 (94 wt.%)–Y_2O_3 (4 wt.%)–Al_2O_3 (2 wt.%), respectively. The composition of SNYb corresponds to the Si_3N_4–$Yb_2Si_2O_7$ tie line.[14] The powder mixtures were milled in methanol for 24 h using Si_3N_4 balls. The milled slurry was dried, sieved, and gas pressure sintered at 1750°C for 2 h under 12 MPa of nitrogen pressure and subsequently annealed at 1950°C for 4 h under 30 MPa of nitrogen pressure.

Densities were measured using Archimedes method. The theoretical densities of the specimens were calculated according to the rule of mixtures. X-ray diffractometry (XRD) was used for ground powders. The sintered specimens were cut, polished, and then plasma-etched by CF_4 containing 7.8% O_2. The microstructures were observed by scanning electron microscopy (SEM). Thin foils for high resolution transmission electron microscopy (HRTEM, Philips CM30, Eindhoven, The Netherlands) were prepared by the standard procedures of grinding, dimpling, and ion-beam thinning followed by carbon coating to minimize charging during the observation of IGF.

Specimens for SCG tests were cut and polished to rectangular bars in a dimension of 3×4×25 mm. Constant stress-rate testing was performed using three-point bend fixture with a span of 15 mm at 1400°C in air. Five or six different speed rates from 10^{-2} to 10^3 MPa/s were employed using a position-controlled mode. A total of ~50 specimens for each composition was tested and the average data obtained from the five specimens were used for the subsequent SCG analysis as described in ASTM standard C 1368.

3. Results and discussion

Relative densities of higher than 98% were obtained for both SNYb and SNAY. SEM micrographs of polished and etched surfaces are shown in Fig. 1. As shown, both have a typical in situ toughened microstructure of Si_3N_4.[16] Fig. 2 shows the XRD analysis of SNYb and SNAY. It shows that the secondary crystalline phase for SNYb is $Yb_4Si_2N_2O_7$, which is not the expected compound in the Si_3N_4–$Yb_2Si_2O_7$ tie-line composition, however, is the compound in the Si_3N_4–$Yb_4Si_2N_2O_7$ tie-line composition.[17] Earlier study[14] showed that hot-pressing with this composition results in $Yb_2Si_2O_7$ as secondary crystalline phase. This difference seems to be originated from the high nitrogen pressure (30 MPa in this study) during sintering, which increases the solubility of nitrogen for the liquid phase. The solubility of nitrogen decreases with decreasing temperature and, therefore, the dissolved nitrogen may participate into the formation of a crystalline phase during cooling. In contrast, a secondary crystalline phase is not detected for SNAY, which indicates that crystallization has not readily occurred in SNAY composition.

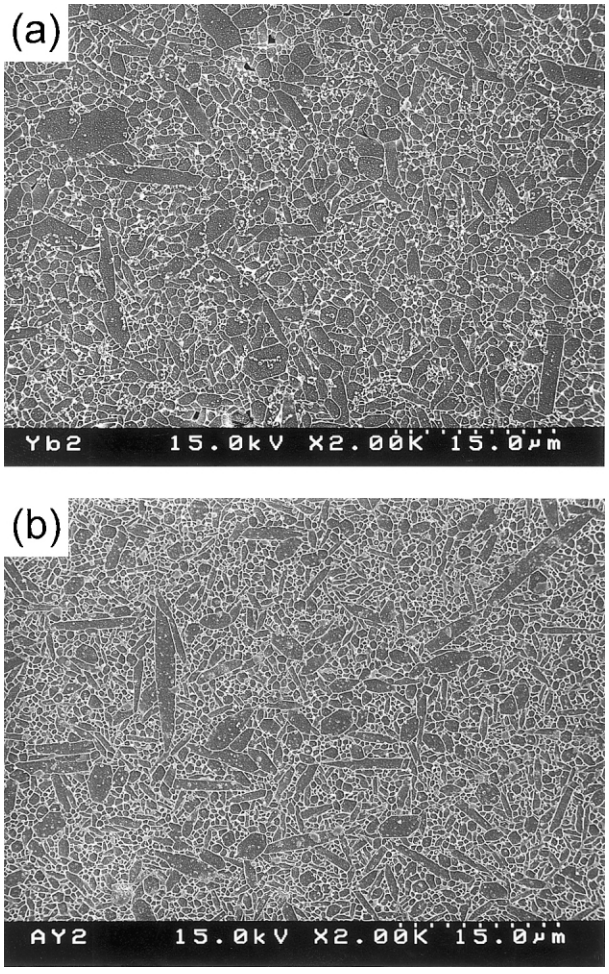

Fig. 1. Typical microstructures for (a) Si_3N_4 with $Yb_2Si_2O_7$ composition and (b) Si_3N_4 with 2 wt.% Al_2O_3 and 4 wt.% Y_2O_3.

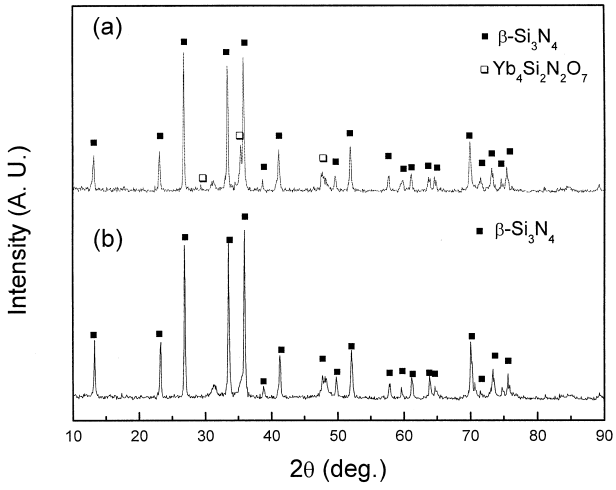

Fig. 2. XRD patterns for (a) Si_3N_4 with $Yb_2Si_2O_7$ composition and (b) Si_3N_4 with 2 wt.% Al_2O_3 and 4 wt.% Y_2O_3.

The results of constant stress-rate testing for SNYb and SNAY at 1400°C are shown in Fig. 3, where log σ_f (fracture strength) was plotted as a function of log $\dot{\sigma}$ (stress rate). The room temperature strengths were arbitrarily plotted for comparison at $\dot{\sigma} = 10^4$ MPa/s. Both SNYb and SNAY exhibited an increase in strength with stress rate. The value of SCG parameter, n, for SNYb and SNAY was determined by a linear regression analysis using the mean strength data. The resulting n was 14.7 and 6.3 for SNYb and SNAY, respectively. To better represent the strength degradation, the strengths at 1400°C were normalized with respect to the corresponding room temperature strength, to give a reduced strength, σ_r. The σ_r is defined as follows:[18]

$$\sigma_r = \frac{\sigma_{f/HT}}{\sigma_{f/RT}} \quad (1)$$

where $\sigma_{f/HT}$ and $\sigma_{f/RT}$ are elevated and room-temperature strengths, respectively. The resulting plot of log σ_r as a function of log $\dot{\sigma}$ is shown in Fig. 4. It indicates that the strength increases from the slow stress test rate (of the order of 10^{-2} MPa/s) to fast stress rate (of the order of 10^3 MPa/s). σ_r increased from 0.29 to 0.55 for SNYb (90% increased) and from 0.10 to 0.31 for SNAY (210% increased). Figs. 3 and 4 indicate that SNYb has better slow crack growth resistance than SNAY.

The elevated-temperature slow crack growth was known as a rate-dependent process occurring by viscous flow of the IGF.[19,20] The viscous flow behavior of IGF is predominantly determined by its refractoriness. The refractory nature can be estimated from the eutectic temperature of sintering additive oxide–SiO_2 system[11,12] and cationic size of sintering additives if the cation act as a network modifier in the SiO^{-4} network structure of IGF.[14,15] The eutectic temperature of the Yb_2O_3–SiO_2 system (1650°C) is higher than that of the Al_2O_3–Y_2O_3–SiO_2 system (<1505°C). The ionic radius of Yb^{3+} (0.985×10^{-1} nm) is smaller than that of Y^{3+} (1.011×10^{-1} nm) (The ionic radius of Al^{3+}, 0.390×10^{-1} nm, is much smaller than that of Yb^{3+} and, therefore, more refractory nature could be expected with addition of Al_2O_3. However, unlikely Yb^{3+} or Y^{3+}, Al^{3+} is incorporated not as modifier but as network former in the IGF structure and greatly weakens the structure and refractoriness). Therefore, the more refractory nature of IGF could be expected for SNYb.

A tie-line composition could also contribute to the refractory nature of IGF for SNYb. A recent study on the diffusive interface description of IGF indicates that there is a "chemical" driving force, which depends on the difference in solute concentration between the liquid phase and the crystalline Si_3N_4 phase, reducing the thickness of IGF and, ultimately, depleting of the IGF in the selective compositions.[21] It has also been reported that the creep resistance, which is also a rate-dependent process occurring by viscous flow of the IGF, of Si_3N_4 ceramics is high when the composition is at the tie-line.[11] Since the creep resistance is mainly controlled by the presence of IGF, it may show a maximum when the grain boundaries are free of IGF. This means that a strong chemical driving force, which can exclude the effect of IGF on the high temperature properties, could be expected at the tie-line composition. Furthermore, readily crystallization of a secondary crystalline phase at triple-junctions, which contributes to better refractoriness of IGF, and high temperature properties can be expected at the tie-line composition.[3,11,12]

Fig. 5 shows the IGF of SNYb and SNAY observed by HRTEM. The IGF for SNYb is narrower (~1 nm) compared to that of SNAY (~1.5 nm). It may be due to the following two factors: (1) the chemical driving force

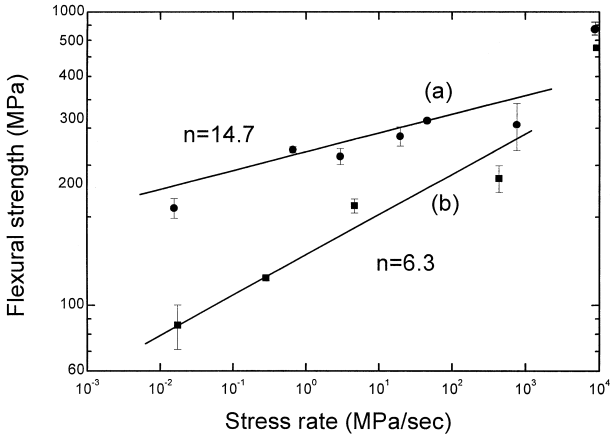

Fig. 3. Plots of 1400°C strength (σ_f) vs stress rate ($\dot{\sigma}$) for (a) Si_3N_4 with $Yb_2Si_2O_7$ composition and (b) Si_3N_4 with 2 wt.% Al_2O_3 and 4 wt.% Y_2O_3. The room temperature strengths were arbitrarily plotted at $\sigma = 10^4$.

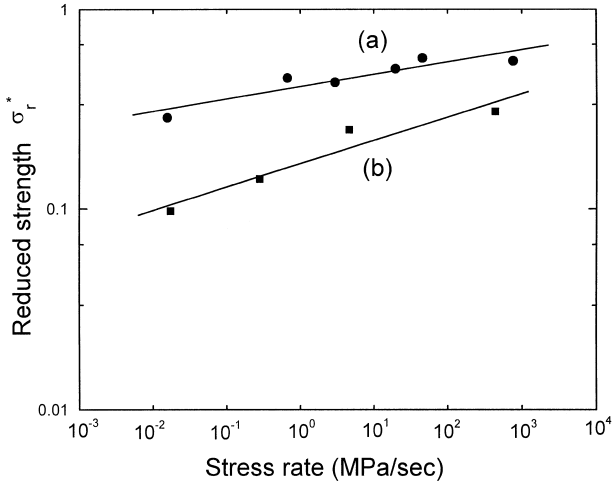

Fig. 4. Plots of reduced strength (σ_r) vs stress rate ($\dot{\sigma}$) for (a) Si_3N_4 with $Yb_2Si_2O_7$ composition and (b) Si_3N_4 with 2 wt.% Al_2O_3 and 4 wt.% Y_2O_3.

for SNYb is stronger than that of SNAY since it has at tie-line composition; (2) most Al^{3+} and Y^{3+} ions may be remained in the IGF since secondary phase containing both ions is not readily crystallized for SNAY. In contrast, the $Yb_4Si_2N_2O_7$ phase is readily crystallized (Fig. 2), which means that most of the Yb^{3+} ions are incorporated in the formation of a crystalline phase. It can contribute to the narrow IGF thickness since the cations of sintering additives widen the thickness of IGF.[22] The two factors contribute to a narrow thickness of IGF also contribute to the superior refractory nature of IGF and better slow crack growth resistance since the former excludes the effect of IGF on the high temperature and the latter results in a silica-rich composition of IGF that has superior refractory nature.[23]

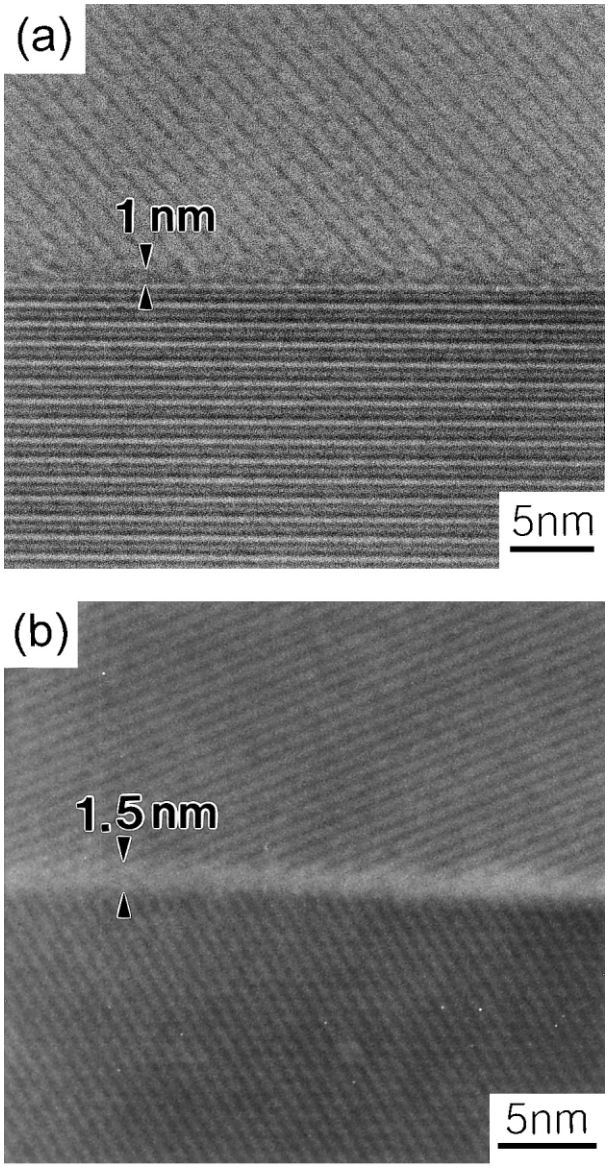

Fig. 5. Representative HRTEM micrographs of grain boundaries for (a) Si_3N_4 with $Yb_2Si_2O_7$ composition and (b) Si_3N_4 with 2 wt.% Al_2O_3 and 4 wt.% Y_2O_3.

4. Summary

Slow crack growth behavior of two kinds of Si_3N_4 ceramics using constant stress rate testing showed that Si_3N_4 with $Yb_2Si_2O_7$ tie-line composition as sintering additives has better slow crack growth resistance, compared to Si_3N_4 with Al_2O_3–Y_2O_3 composition as sintering additives. It was inferred that (i) high eutectic temperature of Yb_2O_3–SiO_2 system, (ii) small cationic radius of Yb^{3+} ion, (iii) strong "chemical driving force" at tie-line composition and (iv) easy crystallization of Yb-containing secondary crystalline phase may contribute to the highly refractory nature of the intergranular glassy film and result in better resistance to slow crack growth.

References

1. Isoke, J. L., Lange, F. F. and Diaz, E. S., Effect of selected impurities on the high temperature mechanical properties of hot-pressed silicon nitride. *J. Mater. Sci.*, 1976, **11**, 908–912.
2. Singhal, J. S. C., Thermodynamics and kinetics of oxidation of hot-pressed silicon nitride. *J. Mater. Sci.*, 1976, **11**, 500–509.
3. Cinibulk, M. K. and Thomas, G., Fabrication and secondary-phase crystallization of rare-earth disilicate-silicon nitride ceramics. *J. Am. Ceram. Soc.*, 1992, **75**, 2037–2043.
4. Hwang, C. J., Fuller, S. M. and Beaman, D. R., Development of a high-performance Si_3N_4 material using transient-liquid-phase and self-reinforcing technology. *Ceram. Engng Sci. Proc.*, 1994, **15**, 685–693.
5. Thompson, D. P., New grain-boundary phases for nitrogen ceramics. In *Proceedings of the Material Research Society Symposium*, ed. I. W. Chen, P. F. Becher, M. Mitomo, G. Petzow and T. S. Tien. Material Research Society, Pittsburgh, 1993, pp. 79–92.
6. Hoffman, M. J. and Petzow, G., Microstructural design of Si_3N_4 based ceramics. In *Proceedings of the Material Research Society Symposium*, ed. I. W. Chen, P. F. Becher, M. Mitomo, G. Petzow and T. S. Tien. Material Research Society, Pittsburgh, 1993, pp. 3–14.
7. Lange, F. F., Singhal, S. C. and Kuznicki, R. C., Phase relationship and stability studies in the Si_3N_4-SiO_2-Y_2O_3 pseudoternary system. *J. Am. Ceram. Soc.*, 1977, **60**, 249–252.
8. Lange, F. F., Si_3N_4–CeO_2–SiO_2 materials: phase relationships and strength. *Am. Ceram. Soc. Bull.*, 1980, **59**, 239–249.
9. Sanders, W. A. and Mieskowski, D. M., Strength and microstructure of sintered Si_3N_4 with rare-earth oxide addition. *Am. Ceram. Soc. Bull.*, 1985, **64**, 304–309.
10. Hirosaki, N., Okada, A. and Matoba, K., Sintering of Si_3N_4 with the addition of rare-earth oxides. *J. Am. Ceram. Soc.*, 1988, **71**, C144–C147.
11. Cinibulk, M. K., Thomas, G. and Johnson, S. M., Strength and creep behavior of rare-earth disilicate-silicon nitride ceramics. *J. Am. Ceram. Soc.*, 1992, **75**, 2050–2055.
12. Cinibulk, M. K. and Thomas, G., Oxidation behavior of rare-earth disilicate-silicon nitride ceramics. *J. Am. Ceram. Soc.*, 1992, **75**, 2044–2049.
13. Morgan, P. E. D., Lange, F. F., Clarke, D. R. and Davis, B. I., A new Si_3N_4 material: phase relations in the system Si-Sc-O-N and preliminary property studies. *J. Am. Ceram. Soc.*, 1981, **64**, C77–C78.
14. Choi, H. J., Lee, J. G. and Kim, Y.-W., High temperature strength and oxidation behaviour of hot-pressed silicon nitride-disilicate ceramics. *J. Mater. Sci.*, 1997, **32**, 1937–1942.

15. Choi, H. J., Lee, J. G. and Kim, Y.-W., Oxidation behavior of hot-pressed Si_3N_4 with Re_2O_3 (Re = Y, Yb, Er, La). *J. Eur. Ceram. Soc.*, 1999, **19**, 2757–2762.
16. Mitomo, M. and Uenosono, S., Microstructural development during gas-pressure sintering of α-Si_3N_4. *J. Am. Ceram. Soc.*, 1992, **75**, 103–108.
17. Nishimura, T. and Mitomo, M., Phase relationship in the Si_3N_4–SiO_2–Yb_2O_3. *J. Mater. Res.*, 1995, **10**, 240–242.
18. Choi, S. R. and Salem, J. A., Ultra-fast fracture strength of advanced ceramics at elevated temperature. *Mater. Sci. Proc.*, 1996, **A242**, 129–136.
19. Tighe, N. J., The structure of slow crack growth interfaces in silicon nitride. *J. Mater. Sci.*, 1978, **13**, 1455–1463.
20. Tasi, R. L. and Raj, R., The role of grain-boundary sliding in fracture of hot-pressed Si_3N_4 at high temperature. *J. Am. Ceram. Soc.*, 1980, **63**, 4–7.
21. Bobeth, M., Clarke, D. R. and Pompe, W., A diffusive interface description of intergranular films in polycrystalline ceramics. *J. Am. Ceram. Soc.*, 1999, **82**, 1537–1546.
22. Wang, C. M., Pan, X., Hoffman, M. J., Cannon, R. M. and Rühle, M., Grain boundary films in rare-earth-glass-based silicon nitride. *J. Am. Ceram. Soc.*, 1996, **79**, 788–792.
23. Klemn, H. and Pezzotti, G., Fracture toughness and time-dependent strength behavior of low-doped silicon nitride for applications at 1400°C. *J. Am. Ceram. Soc.*, 1994, **77**, 553–561.